Oxotungsten(VI) Chemistry of Hydrotris(3,5-dimethylpyrazol-1-yl)borate: Hydroxodioxotungsten(VI), Trioxotungsten(VI), and (μ-Oxo)bis[dioxotungsten(VI)] Complexes

Aston A. Eagle,[1a] Graham N. George,[1b] Edward R. T. Tiekink,[1c] and Charles G. Young*,[1a]

School of Chemistry, University of Melbourne, Parkville, Victoria 3052, Australia, Stanford Synchrotron Radiation Laboratory, SLAC, P.O. Box 4349, MS 69, Stanford, California 94309, and Department of Chemistry, University of Adelaide, Adelaide, South Australia 5005, Australia

Received August 1, 1996[⊗]

Colorless, diamagnetic, air-stable $LW^{VI}O_2(OH)$ [L = hydrotris(3,5-dimethylpyrazol-1-yl)borate] forms when suspensions of $LW^{II}I(CO)_3$ in dimethyl sulfoxide are heated at 100 °C. The complex was characterized by microanalysis, high-resolution mass spectrometry, and IR, NMR, and EXAFS spectroscopic techniques. The complex behaves as a weak acid with a pK_a of around 4.7. Reaction of $LWO_2(OH)$ with NEt_4OMe results in the formation of colorless, diamagnetic, air-stable $NEt_4[LW^{VI}O_3]$, which crystallizes as a tetrahydrate. Crystals of $NEt_4[LWO_3]\cdot 4H_2O$ are monoclinic, space group $P2_1/c$, with $a = 18.804(4)$ Å, $b = 9.901(8)$ Å, $c = 17.447(3)$ Å, $\beta = 104.35(2)°$, and $V = 3146(1)$ Å^3 for $Z = 4$. The structure is composed of discrete NEt_4^+ and *fac*-$[LWO_3]^-$ ions strung in an alternating fashion along both sides of a zigzag ladder of hydrogen-bonded water molecules (directed parallel to the *b* axis). The distorted-octahedral $[LWO_3]^-$ anions, with W−O(1) = 1.740(4) Å, W−O(2) = 1.759(4) Å, and W−O(3) = 1.765(4) Å, are hydrogen-bonded to water molecules through two oxo groups, with WO(2)··O(5)^i = 2.666(6) Å and WO(3)··O(4)^{ii} = 2.693(6) Å. The EXAFS spectra of $NEt_4[LWO_3]\cdot 4H_2O$ and $LWO_2(OH)$ and related complexes are diagnostic of the respective trioxo or hydroxo−dioxo centers present. Colorless, diamagnetic, air-stable $[LW^{VI}O_2]_2(\mu\text{-}O)$ is produced in a number of reactions, including the oxidation of $LW^{VI}O_2(\mu\text{-}O)W^{IV}O(CO)L$ and metathesis reactions involving $LW^{VI}O_2Cl$. The complex exhibits NMR spectra consistent with molecular C_2 symmetry and IR bands assignable to $\nu(WO_2)$ (945 and 900 cm^{-1}) and $\nu_{as}(WOW)$ (780 cm^{-1}) vibrational modes. Crystals of $[LW^{VI}O_2]_2(\mu\text{-}O)$ are monoclinic, space group $C2/c$, with $a = 28.112(7)$ Å, $b = 9.538(7)$ Å, $c = 15.722(8)$ Å, $\beta = 115.56(2)°$, and $V = 3802(3)$ Å^3 for $Z = 4$. The dinuclear structure is composed of distorted-octahedral LWO_2 units linked by the μ-oxo ligand; the terminal W═O bond lengths are identical at 1.715(5) Å, while the bridging W−O(3) distance is 1.893(1) Å.

Introduction

Collectively, the early transition metals form innumerable oxides,[2] oxometalate anions,[3] and mono- and polynuclear oxo complexes;[4−6] these have many roles in industrial and biological catalytic systems. However, relatively few mononuclear *fac* trioxo−metal complexes have been reported, and these are largely restricted to the elements molybdenum, tungsten, technetium, and rhenium.[4,5] The rarity of *fac* trioxo−metal complexes, their potential as oxidation and olefin metathesis catalysts,[7,8] and their recent detection in biological systems[9] have stimulated interest in their chemistry. Our interest in the high-valent chemistry of tungsten and its role in biochemistry[10−12] has led to the discovery of a number of oxotungsten(VI) complexes containing the hydrotris(3,5-dimethylpyrazol-1-yl)-borate ligand, L;[13−19] here, we report the synthesis and characterization of $LW^{VI}O_2(OH)$, $NEt_4[LW^{VI}O_3]\cdot 4H_2O$, and $[LW^{VI}O_2]_2(\mu\text{-}O)$, a tungsten L_{III}-edge EXAFS study of $LWO_2(OH)$, $NEt_4[LWO_3]\cdot 4H_2O$, and related complexes, and the crystal structures of $NEt_4[LWO_3]\cdot 4H_2O$ and $[LWO_2]_2(\mu\text{-}O)$. Monomeric *fac* trioxotungsten(VI) complexes are rare and

⊗ Abstract published in *Advance ACS Abstracts,* January 1, 1997.

(1) (a) University of Melbourne. (b) Stanford Synchrotron Radiation Laboratory. (c) University of Adelaide.
(2) Wells, A. F. *Structural Inorganic Chemistry*, 5th ed.; Clarendon Press: Oxford, U.K., 1984.
(3) Pope, M. T. *Heteropoly and Isopoly Oxometalates*; Springer-Verlag: Berlin, 1983.
(4) Griffith, W. P. *Coord. Chem. Rev.* **1970**, *5*, 459.
(5) Nugent, W. A.; Mayer, J. M. *Metal-Ligand Multiple Bonds*; Wiley: New York, 1988.
(6) West, B. O. *Polyhedron* **1989**, *8*, 219.
(7) Sheldon, R. A.; Kochi, J. K. *Metal-Catalysed Oxidation of Organic Compounds*; Academic: New York, 1981.
(8) (a) Herrmann, W. A.; Kuchler, J. G.; Felixberger, J. K.; Herdtweck, E.; Wagner, W. *Angew. Chem., Int. Ed. Engl.* **1988**, *27*, 394. (b) Herrmann, W. A.; Wagner, W.; Flessner, U. N.; Volkhardt, U.; Komber, H. *Angew. Chem., Int. Ed. Engl.* **1991**, *30*, 1636. (c) Herrmann, W. A.; Fischer, R. W.; Marz, D. W. *Angew. Chem., Int. Ed. Engl.* **1991**, *30*, 1638. (d) Herrmann, W. A.; Wang, M. *Angew. Chem., Int. Ed. Engl.* **1991**, *30*, 1641. (e) Herrmann, W. A.; Fischer, R. W.; Rauch, M. U.; Scherer, W. *J. Mol. Catal.* **1994**, *86*, 243.
(9) George, G. N.; Garrett, R. M.; Prince, R. C.; Rajagopalan, K. V. *J. Am. Chem. Soc.* **1996**, *118*, 8588.
(10) Adams, M. W. W. *Annu. Rev. Microbiol.* **1993**, *47*, 627.
(11) Adams, M. W. W. In *Encyclopedia of Inorganic Chemistry*; King, R. B., Ed.; Wiley: Chichester, U.K., 1994; Vol. 8, p 4284.
(12) Enemark, J. H.; Young, C. G. *Adv. Inorg. Chem.* **1993**, *40*, 1.
(13) Young, C. G.; Gable, R. W.; Mackay, M. F. *Inorg. Chem.* **1990**, *29*, 1777.
(14) (a) Eagle, A. A.; Tiekink, E. R. T.; Young, C. G. *J. Chem. Soc., Chem. Commun.* **1991**, 1746. (b) Eagle, A. A.; Young, C. G.; Tiekink, E. R. T. *Organometallics* **1992**, *11*, 2934.
(15) Eagle, A. A.; Harben, S. M.; Tiekink, E. R. T.; Young, C. G. *J. Am. Chem. Soc.* **1994**, *116*, 9749.
(16) Thomas, S.; Tiekink, E. R. T.; Young, C. G. *Organometallics* **1996**, *15*, 2428.
(17) Eagle, A. A.; Thomas, S.; Young, C. G. In *Transition Metal Sulfur Chemistry: Biological and Industrial Significance;* ACS Symposium Series No. 653; American Chemical Society: Washington, DC, 1996; Chapter 20, p 324.
(18) Eagle, A. A. Ph.D. Dissertation, University of Melbourne, 1996.
(19) Abbreviations: L = hydrotris(3,5-dimethylpyrazol-1-yl)borate; dien = diethylenetriamine; tcn = 1,4,7-triazacyclononane; Me_3tcn = 1,4,7-trimethyl-1,4,7-triazacyclononane; Cp* = η^5-pentamethylcyclopentadienyl; $HB(pz)_3^-$ = hydrotripyrazolylborate; XAS = X-ray absorption spectroscopy; EXAFS = Extended X-ray absorption fine structure.

S0020-1669(96)00926-3 CCC: $14.00

include $[WO_3S]^{2-}$,[20] (dien)WO_3,[21] $[WO_3(CH_2CMe_3)]^-$,[22] (tcn)WO_3 and (Me$_3$tcn)WO_3,[23−25] $[Cp^*WO_3]^-$,[26,27] and $[LWO_3]^-$.[28] Moreover, very few well-characterized hydroxodioxotungsten(VI) and (μ-oxo)bis[dioxotungsten(VI)] complexes are known to exist.[24−26,29−33]

Experimental Section

Materials and Methods. Potassium hydrotris(3,5-dimethylpyrazol-1-yl)borate (KL),[34] LWI(CO)$_3$,[35] LWO$_2$(μ-O)WO(CO)L,[13] LWO$_2$(OMe),[18] (dien)WO_3,[21] (Me$_3$tcn)WO_3,[23,25] and [(Me$_3$tcn)-WO_2(OH)]Br[25] were prepared by literature methods or slight modifications thereof. All other reagents were AR grade or higher. Infrared spectra were recorded on a Perkin-Elmer 1430 spectrophotometer as pressed KBr disks. NMR spectra were obtained using a Varian FT Unity-300 spectrometer and were referenced to internal $CHCl_3$ (δ 7.26). High-resolution mass spectra were recorded using a VG7070F instrument referenced against $C_{13}F_{19}$ (*m*/*z* 516.969657).[36] Electrochemical experiments were performed using a Cypress Electrochemical System II with a 3 mm glassy carbon working electrode and platinum auxiliary and reference electrodes. Solutions of LWO$_2$(OH) (1−2 mM) in 0.1 M NBu$^n_4$BF$_4$/acetonitrile were employed, and potentials were referenced to internal ferrocene at +0.390 V vs a saturated calomel electrode (SCE). Potentials are reported relative to the SCE. Microanalyses were performed by Atlantic Microlabs, Norcross, GA.

Syntheses and Characterization Data. LWO$_2$(OH). A suspension of LWI(CO)$_3$ (2.81 g, 4.06 mmol) in dimethyl sulfoxide (10 mL) was stirred in air at 100 °C for 12 min (*caution! gas evolution*) and then allowed to cool. Acetonitrile (25 mL) was added, and after a brief period of stirring, the mixture was filtered and the isolated solid was washed with acetonitrile (10 mL). The product is generally very pure at this point, but analytically pure white microcrystals may be obtained by dissolving the crude product in warm 1:1 CH_2Cl_2/methanol followed by volume reduction and precipitation with acetonitrile. Yield: 1.77 g (83%). The analogous deuterated complex, LWO$_2$(OD), was prepared by the addition of a DCl/D$_2$O solution to a solution of NEt$_4$-[LWO$_3$]·4H$_2$O in dry acetonitrile.

Anal. Calcd for $C_{15}H_{23}BN_6O_3W$: C, 33.99; H, 4.37; N, 15.86. Found: C, 34.14; H, 4.44; N, 15.90. IR (KBr): ν(OH) 3270 m br, 2930 m, ν(BH) 2535 m, 1540 s, 1490 w, 1445 s, 1410 s, 1385 s, 1365 s, 1205 s, 1185 s, 1070 s, 1045 s, 985 w, ν(WO$_2$) 945 s and 895 s, 860 s, 810 s, 785 m, 690 s, 670 s, 650 s, 470 m, 375 m cm^{-1}. ^{1}H NMR ($CDCl_3$): δ 2.36 (9H), 2.70 (9H), 5.88 (3H). Mass spectrum: [M]$^+$, *m*/*z* 530 (8%); [M − H$_2$O]$^+$, *m*/*z* 512 (20%); [M − Me$_2$C$_5$HN$_2$]$^+$, *m*/*z* 433 (35%). Cyclic voltammetry (MeCN, vs SCE): E_{pc} = −1.50 V (irreversible, W^{VI}/W^{V}); E_{pc} = −1.74 V (irreversible).

NEt$_4$[LWO$_3$]·4H$_2$O. A stock solution of NEt$_4$OMe was prepared by adding 0.50 mL of a 25% w/w aqueous NEt$_4$OH solution to methanol (14.0 mL) and then adding acetonitrile up to the mark of a 50.00 mL standard flask. Treatment of an acetonitrile (5 mL) suspension of LWO$_2$(OH) (0.100 g, 0.189 mmol) with this solution (11.7 mL, 0.2 mmol) led over 30 s to a colorless solution, which, after being stirred for 40 min, was evaporated to dryness. The residue was dissolved in CH_2Cl_2 (1 mL), and diethyl ether (5 mL) was added dropwise to precipitate white crystals. The mixture was reduced in volume, and more diethyl ether was added. Yield: 0.127 g (92%).

Anal. Calcd for $C_{23}H_{50}BN_7O_7W$: C, 37.77; H, 6.89; N, 13.41. Found: C, 37.85; H, 6.92; N, 13.17. IR (KBr): 2970 m, 2920 m, ν(BH) 2520 m, ν(NEt$_4^+$) 1645 br m, 1535 s, 1485 m, 1445 s, 1415 s, 1385 s, 1375 s, 1205 s, ν(NEt$_4^+$) 1185 s, 1170 m, 1065 s, 1045 s, 1000 w, ν(WO$_3$) 920 s and 860 vs and 825 vs, 800 s, 780 m, 695 m, 645 m, 470 w, 370 w, 345 w cm^{-1}. IR ($CHCl_3$): ν(WO$_3$) 920 m and 840 vs cm^{-1}. ^{1}H NMR ($CDCl_3$): δ 1.43 (tt, 12H, *J* = 7.5 Hz), 2.05 (8H of H$_2$O), 2.28 (9H), 2.83 (9H), 3.54 (q, 8H, *J* = 7.5 Hz), 5.72 (3H). Mass spectrum (FAB, thioglycerol): {(NEt$_4$)$_2$[LWO$_3$]}$^+$, *m*/*z* 789 (5%). Cyclic voltammetry (MeCN, vs SCE): no process observed.

[LWO$_2$]$_2$(μ-O). Treatment of a stirred solution of LWO$_2$(μ-O)-WO(CO)L (0.058 g, 0.055 mmol) in chloroform (10 mL) with *tert*-butyl hydroperoxide (0.50 mL of a 3.0 M toluene solution, 1.5 mmol) and then iodine (0.025 g, 0.197 mmol) led to the rapid development of an orange solution. This was stirred for 0.5 h and then reduced to dryness. The residue was recrystallized from dichloromethane/methanol. Slow diffusion of methanol into a dichloromethane solution of the product produced pale yellow crystals. Yield: 0.020 g (35%).

Anal. Calcd for $C_{30}H_{44}B_2N_{12}O_5W_2$: C, 34.57; H, 4.26; N, 16.13. Found: C, 34.35; H, 4.21; N, 15.92. IR (KBr): 2930 w, ν(BH) 2545 w, 1540 s, 1445 s, 1415 s, 1380 s, 1365 s, 1210 s, 1185 w, 1070 s, 1045 s, 985 w, ν(WO$_2$) 945 s and 900 s, 860 w, 810 s, ν_{as}(WOW) 780 vs, 690 w, 640 m, 595 w br, 470 w, 425 w, 380 w cm^{-1}. ^{1}H NMR ($CDCl_3$): δ 1.10 (6H), 2.29 (6H), 2.35 (6H), 2.36 (6H), 2.77 (6H), 3.22 (6H), 5.44 (2H), 5.81 (2H), 5.92 (2H). Mass spectrum (FAB, thioglycerol): [M]$^+$, *m*/*z* 1042 (4%). EI: [M]$^+$, *m*/*z* 1042 (18%).

Crystal Structure of NEt$_4$[LWO$_3$]·4H$_2$O. Crystals of NEt$_4$-[LWO$_3$]·4H$_2$O were grown by diffusion of hexane into a solution of the compound in dichloromethane. Intensity data for a pale yellow plate (0.07 × 0.24 × 0.24 mm) were measured at room temperature (20 °C) on a Rigaku AFC6R diffractometer fitted with graphite-monochromatized Mo Kα radiation, λ = 0.710 73 Å; the ω−2θ scan technique was employed to measure 6148 data (5946 unique) such that $2\theta_{max}$ was 50.0°. No decomposition of the crystal occurred during the data collection, and 3899 absorption-corrected (range of transmission factors 0.982−1.015) data[37] which satisfied the $I \geq 3.0\sigma(I)$ criterion were used in the subsequent analyses. Crystal data are given in Table 1.

The structure was solved by direct methods[38] and refined by a conventional full-matrix least-squares procedure based on *F*.[39] Non-hydrogen atoms were refined with anisotropic thermal parameters, and H atoms were included in the model at their calculated positions (C−H 0.97 Å); the water hydrogen atoms were not located in the analysis. At convergence [σ weights, i.e. $1/\sigma^2(F)$], R = 0.030 and R_w = 0.032; final refinement details are given in Table 1. The analysis of variance showed no special features, no correction was made for extinction effects, and the maximum peak in the final difference map was 0.58 e Å^{-3}. Scattering factors for all atoms were those incorporated in the teXsan program.[39] The crystallographic numbering scheme is shown in Figure 1, which was drawn with the ORTEP program[40] at the 30% probability level.

(20) (a) Diemann, E.; Müller, A. *Coord. Chem. Rev.* **1973**, *10*, 79. (b) Müller, A.; Diemann, E.; Jostes, R.; Bögge, H. *Angew. Chem., Int. Ed. Engl.* **1981**, *20*, 934.
(21) Taylor, R. S.; Gans, P.; Knowles, P. F.; Sykes, A. G. *J. Chem. Soc., Dalton Trans.* **1972**, 24.
(22) (a) Feinstein-Jaffe, I.; Pedersen, S. F.; Schrock, R. R. *J. Am. Chem. Soc.* **1983**, *105*, 7176. (b) Feinstein-Jaffe, I.; Dewan, J. C.; Schrock, R. R. *Organometallics* **1985**, *4*, 1189.
(23) Roy, P. S.; Wieghardt, K. *Inorg. Chem.* **1987**, *26*, 1885.
(24) Schreiber, P.; Wieghardt, K.; Nuber, B.; Weiss, J. *Polyhedron* **1989**, *8*, 1675.
(25) Schreiber, P.; Wieghardt, K.; Nuber, B.; Weiss, J. *Z. Anorg. Allg. Chem.* **1990**, *587*, 174.
(26) (a) Rau, M. S.; Kretz, C. M.; Mercando, L. A.; Geoffroy, G. L. *J. Am. Chem. Soc.* **1991**, *113*, 7420. (b) Rau, M. S.; Kretz, C. M.; Geoffroy, G. L.; Rheingold, A. L. *Organometallics* **1993**, *12*, 3447.
(27) Sundermeyer, J.; Radius, U.; Burschka, C. *Chem. Ber.* **1992**, *125*, 2379.
(28) Sundermeyer, J.; Putterlik, J.; Pritzkow, H. *Chem. Ber.* **1993**, *126*, 289.
(29) Chaudhuri, P.; Wieghardt, K.; Tsai, Y.-H.; Krüger, C. *Inorg. Chem.* **1984**, *23*, 427.
(30) Chaudhuri, P.; Wieghardt, K.; Gebert, W.; Jibril, I.; Huttner, G. *Z. Anorg. Allg. Chem.* **1985**, *521*, 23.
(31) Griffith, W. P.; Pumphrey, C. A.; Rainey, T.-A. *J. Chem. Soc., Dalton Trans.* **1986**, 1125.
(32) Llopis, E.; Ramirez, J. A.; Domenech, A.; Cervilla, A. *J. Chem. Soc., Dalton Trans.* **1993**, 1121.
(33) Kläui, W.; Hardt, T.; Schulte, H.-J.; Hamers, H. *J. Organomet. Chem.* **1995**, *498*, 63.
(34) Trofimenko, S. *J. Am. Chem. Soc.* **1967**, *89*, 6288.
(35) Feng, S. G.; Philipp, C. C.; Gamble, A. S.; White, P. S.; Templeton, J. L. *Organometallics* **1991**, *10*, 3504.
(36) All atomic masses used in calculations were taken from: Beynon, J. H.; Williams, A. E. *Mass and Adundance Tables for Use in Mass Spectrometry*; Elsevier: Amsterdam, 1963.
(37) Walker, N.; Stuart, D. *Acta Crystallogr.* **1983**, *A39*, 158.
(38) Burla, M. C.; Camalli, M.; Cascarano, G.; Giacovazzo, C.; Polidori, G.; Spagna, R.; Viterbo, D. *J. Appl. Crystallogr.* **1989**, *22*, 389.
(39) *teXsan: Structure Analysis Package*; Molecular Structure Corp.: The Woodlands, TX, 1992.

Table 1. Crystallographic Data for $NEt_4[LWO_3]\cdot 4H_2O$ and $[LWO_2]_2(\mu\text{-O})$

empirical formula	$C_{23}H_{50}BN_7O_7W$	$C_{30}H_{44}B_2N_{12}O_5W_2$
fw	731.4	1042.1
space group	monoclinic $P2_1/c$	monoclinic $C2/c$
a, Å	18.804(4)	28.112(7)
b, Å	9.901(8)	9.538(7)
c, Å	17.447(3)	15.722(8)
β, deg	104.35(2)	115.56(2)
V, Å^3	3146(1)	3802(3)
Z	4	4
T, °C	20	20
λ, Å	0.7107	0.7107
ρ_{calcd}, g cm^{-3}	1.544	1.820
hkl range collected	$-25 \le h \le 25$	$0 \le h \le 37$
	$0 \le k \le 13$	$0 \le k \le 12$
	$0 \le l \le 23$	$-20 \le l \le 20$
$F(000)$	1488	2024
μ, cm^{-1}	37.24	61.06
no. of data measd	6148	3686
no. of unique data	5946	3606
no. of obsd data, $I \ge 3.0\sigma(I)$	3899	2270
R^a	0.030	0.031
$R_w{}^b$	0.032	0.030

[a] $R = \Sigma||F_o| - |F_c||/\Sigma|F_o|$. [b] $R_w = \Sigma[(|F_o| - |F_c|)w^{1/2}]/\Sigma[|F_o|w^{1/2}]$.

Crystal Structure of $[LWO_2]_2(\mu\text{-O})$. Crystals of $[LWO_2]_2(\mu\text{-O})$ were grown by diffusion of diethyl ether into a chloroform solution of the compound. Data collection and reduction and solution and refinement of the structure were as above for a pale yellow plate (0.05 × 0.16 × 0.32 mm). Of the 3686 data measured, 3606 were unique, and of these, 2270 absorption-corrected data (minimum and maximum transmission factors: 0.960 and 1.025) satisfied the $I \ge 3.0\sigma(I)$ criterion; $R = 0.031$ and $R_w = 0.030$, the maximum peak was 0.68 e Å^{-3}, and the ORTEP diagram (Figure 6) was drawn at the 40% probability level.

X-ray Absorption Spectroscopy. Data Collection. X-ray absorption spectroscopy (XAS) was carried out at the Stanford Synchrotron Radiation Laboratory with the SPEAR storage ring containing 55−90 mA at 3.0 GeV. Tungsten L_{III}-edge X-ray absorption spectra were collected on beamline 7-3 using a Si(220) double-crystal monochromator with an upstream vertical aperture of 1 mm and a wiggler field of 1.8 T. Harmonic rejection was accomplished by detuning one monochromator crystal to approximately 60% off-peak. X-ray absorption was measured in transmittance using nitrogen-filled ionization chambers. A spectrum of tungsten foil was collected simultaneously with that of the sample, and spectra were calibrated with reference to the lowest energy inflection point of the L_{III}-edge, assumed to be 10 207 eV. Samples were prepared in a boron nitride matrix and during data collection were maintained at a temperature of approximately 10 K using an Oxford Instruments liquid-helium-flow cryostat.

Data Analysis. Data were analyzed using the EXAFSPAK[41] suite of computer programs running on Digital Equipment Corp. VAXstation and Alpha graphics workstations. The extended X-ray absorption fine structure (EXAFS) oscillations $\chi(k)$ were quantitatively analyzed by curve-fitting. The EXAFS total amplitude and phase-shift functions were calculated using the program feff of Rehr and co-workers.[42,43] The small outer-shell EXAFS of complexes containing L was modeled using the multiple-scattering capabilities of feff and an idealized facially tridentate ligand structure. The principal structural information derived from the EXAFS analyses are summarized in Table 2.

Results and Discussion

Synthesis and Characterization of $LWO_2(OH)$. When suspensions of brown $LWI(CO)_3$ in dimethyl sulfoxide were heated to 100 °C, effervescence accompanied the formation of a pale yellow precipitate of $LWO_2(OH)$. The same reaction was observed under both anaerobic and aerobic conditions. Recrystallization yielded pure, colorless microcrystals of $LWO_2(OH)$. The compound is indefinitely air-stable in the solid state and solution; it is most soluble in a 1:1 mixture of CH_2Cl_2 and MeOH but is virtually insoluble in water, alcohols, tetrahydrofuran, diethyl ether, chlorinated and aromatic hydrocarbons, and alkanes. Oxidative decarbonylation of $LW^{II}I(CO)_3$ to $LW^{VI}O_2(OH)$ is likely to proceed via two oxygen atom transfer (OAT) reactions involving dimethyl sulfoxide. A requirement for water as the source of the hydroxo ligand is implied by eq 1, where X = I. In this reaction, product HI will react with solvent to form $[Me_2SOH]I$ or Me_2SI_2 and H_2O.[44,45]

$$LW^{II}X(CO)_3 + 2Me_2SO + H_2O \rightarrow LW^{VI}O_2(OH) + 2Me_2S + HX + 3CO \quad (1)$$

The same compound was formed upon thermolysis of dimethyl sulfoxide solutions of $LWH(CO)_3$[46] (eq 1, X = H) or pyridine solutions of $LWI(CO)_3$ in air (eq 2, py = pyridine). The generation of LWOX(CO) and CO_2 upon reaction of $LWI(CO)_3$ with O_2 at room temperature provides a precedent for the first of the two stepwise oxidations implied by eq 2.[47]

$$LW^{II}I(CO)_3 + 2O_2 + H_2O + py \rightarrow LW^{VI}O_2(OH) + pyHI + CO + 2CO_2 \quad (2)$$

Finally, $LWO_2(OH)$ was formed upon hydrolysis of $LWO_2(SePh)$[18] in acetonitrile according to eq 3, a reaction enhanced

Table 2. EXAFS Curve-Fitting Results[a]

compd	*N* atom type	*R*, Å	σ^2, Å^2	E_o, eV	fit error[b]
$NEt_4[LWO_3]\cdot 4H_2O$	3 W=O	1.766(3)	0.0012(2)	−3.6(10)	0.226
	3 W−N	2.314(8)	0.0024(6)		
$(Me_3tcn)WO_3$	3 W=O	1.766(3)	0.0011(2)	−4.8(10)	0.220
	3 W−N	2.354(8)	0.0024(6)		
$(dien)WO_3$[c]	3 W=O	1.775(3)	0.0010(2)	−4.6(12)	0.248
	3 W−N	2.303(10)	0.0025(7)		
$LWO_2(OH)$	2 W=O	1.736(4)	0.0012(2)	−3.7(14)	0.261
	1 W−O	1.903(10)	0.0019(7)		
	3 W−N	2.256(10)	0.0046(8)		
$[(Me_3tcn)WO_2(OH)]Br$	2 W=O	1.731(7)	0.0014(3)	−5.6(20)	0.375
	1 W−O	1.877(18)	0.0026(2)		
	3 W−N	2.321(10)	0.0026(7)		
$LWO_2(OMe)$	2 W=O	1.733(4)	0.0012(2)	−4.4(12)	0.275
	1 W−O	1.898(11)	0.002(1)		
	1 W−N	2.170(14)	0.0011(6)		
	2 W−N	2.308(8)	0.0011(6)		

[a] Coordination number *N*, interatomic distance *R* (Å), and (thermal and static) mean-square deviation in *R* (the Debye−Waller factor) σ^2 (Å^2). The values in parentheses are estimated standard deviations (precisions) obtained from the diagonal elements of the covariance matrix. We note that the accuracies will be somewhat larger than the precisions, typically ±0.02 Å for *R* and ±20% for *N* and σ^2. [b] The fit error is defined as $\Sigma k^6(\chi_{exptl} - \chi_{calcd})^2/\Sigma k^6\chi_{exptl}{}^2$. [c] Strong backscattering from distant tungsten atoms, at approximately 5.15 and 5.86 Å, was observed for this compound.

(40) Johnson, C. K. *ORTEP II*; ORNL Report 5136; Oak Ridge National Laboratory: Oak Ridge, TN, 1976.
(41) This program is available upon request from G.N.G.
(42) Rehr, J. J.; Mustre de Leon, J.; Zabinsky, S. I.; Albers, R. C. *J. Am. Chem. Soc.* **1991**, *113*, 5135.
(43) Mustre de Leon, J.; Rehr, J. J.; Zabinsky, S. I.; Albers, R. C. *Phys. Rev.* **1991**, *B44*, 4146.
(44) Szmant, H. H. In *Organic Sulfur Compounds;* Kharasch, N., Ed.; Pergamon: New York, 1961; Vol. 1, p 154.
(45) Ranky, W. O.; Nelson, D. C. In *Organic Sulfur Compounds;* Kharasch, N., Ed.; Pergamon: New York, 1961; Vol. 1, p 170.
(46) Caffyn, A. J. M.; Feng, S. G.; Dierdorf, A.; Gamble, A. S.; Eldredge, P. A.; Vossen, M. R.; White, P. S.; Templeton, J. L. *Organometallics* **1991**, *10*, 2842.
(47) Feng, S. G.; Luan, L.; White, P.; Brookhart, M. S.; Templeton, J. L.; Young, C. G. *Inorg. Chem.* **1991**, *30*, 2582.

by the lability of the selenophenolate ligand (note: HSePh is unstable and is converted to Ph_2Se_2, which was detected).

$$LWO_2(SePh) + H_2O \rightarrow LWO_2(OH) + HSePh \qquad (3)$$

The formation of $LWO_2(OH)$ contrasts with the isolation of *fac* trioxo−W(VI) complexes by related oxidative and hydrolytic processes. For example, the oxidative decarbonylation of $(tcn)W(CO)_3$ and $(Me_3tcn)W(CO)_3$ produces $(tcn)WO_3$ and $(Me_3tcn)WO_3$, respectively,[23] while the hydrolysis of $W(CCMe_3)(OCMe_3)_3$ and $LWO_2(CHPPh_3)$ produces $[WO_3(CH_2CMe_3)]^-$ [22] and $[LWO_3]^-$,[28] respectively. As well, oxidative decarbonylation of $NEt_4[(HB(pz)_3)Mo(CO)_3]$ with dimethyldioxirane results in the formation of $NEt_4[(HB(pz)_3)MoO_3]\cdot 2H_2O$, which has been crystallographically characterized.[48] The synthesis of $NEt_4[LMoO_3]$ has also been claimed, but complete characterization data are unavailable.[48]

The formula of $LWO_2(OH)$ was established by microanalysis and mass spectrometry. Microanalytical data were consistent with the absence of water or other solvent of crystallization. Low-resolution, electron-impact mass spectrometry revealed peak clusters at *m/z* 530 (8%), 512 (20%), and 433 (35%), which were assigned to $[M]^+$, $[M - H_2O]^+$, and $[M - Me_2C_5HN_2]^+$ ions, respectively. The isotope patterns of the $[M]^+$ and $[M - Me_2C_5HN_2]^+$ clusters were consistent with loss of a hydrogen atom from about 35% of the ions. Similar behavior was not evident in the $[M - H_2O]^+$ peak cluster. High-resolution mass spectrometry established $m/z = 530.1420 \pm 10$ for the most abundant isotopomer of $[M]^+$ [calculated *m/z* 530.141359 for $LWO_2(OH)$]. High-resolution mass spectrometric studies of the analogous deuterated compound, $LWO_2(OD)$, established $m/z = 531.1465 \pm 10$ for the most abundant isotopomer of $[M]^+$ (calculated *m/z* 531.147637). These high-resolution experiments confirm the presence of a single hydroxo proton or deuteron in the $LWO_2(OH)$ and $LWO_2(OD)$ complexes, respectively ($\Delta(m/z) = 1.0045 \pm 20$, calculated 1.0056). The infrared spectrum of $LWO_2(OH)$ in KBr revealed the fingerprint bands characteristic of the L ligand, including ν(BH) and ν(CN) bands at 2535 and 1540 cm^{-1}, respectively, and a broad ν(OH) band at 3270 cm^{-1}. As well, two strong bands were observed at 945 and 895 cm^{-1}; these are assigned to the symmetric and asymmetric stretching modes, respectively, of a *cis*-$[WO_2]^{2+}$ unit. Bands in the 960−935 and 915−900 cm^{-1} regions are typical of closely related LWO_2X complexes.[14,18] Solution-phase IR studies in the ν(WO) region were prohibited by low solubilities in suitable solvents. The IR spectrum of $LWO_2(OD)$ was identical to that of $LWO_2(OH)$ except for the presence of a broad feature at 2420 cm^{-1}, in the region expected for ν(OD) modes.[49] The ^1H NMR spectrum of $LWO_2(OH)$ exhibited three resonances (3H,9H,9H), attributable to the methyl (two sets) and methine groups of L in a molecule with effective C_{3v} symmetry. No resonance assignable to the hydroxo ligand proton was observed even in carefully dried chloroform, and the integrations of all observed resonances remained constant upon addition of D_2O to solutions of $LWO_2(OH)$. Fast intermolecular proton exchange, facilitated by the equilibrium shown in eq 4, is consistent with the observed NMR spectrum.

$$LWO_2(OH) + H_2O \rightleftharpoons H_3O^+ + [LWO_3]^- \qquad (4)$$

In the absence of intermolecular exchange, effective C_{3v} symmetry on the NMR time scale could be achieved by rapid intramolecular exchange, envisaged as the rapid hopping of the proton between oxo groups. The potential involvement of hydrolytic processes in this proton exchange has not been explored but is also a possibility.[50] The formulation of the compound as a hydroxodioxotungsten(VI) species is consistent with the EXAFS results presented later.

We have made a qualitative assessment of the Brønsted acidity of $LWO_2(OH)$, through deprotonation and solubilization of the complex upon reaction with a variety of bases, B^-, according to eq 5.

$$LWO_2(OH)(s) + B^- \rightleftharpoons BH + [LWO_3]^-(soln) \qquad (5)$$

Suspensions of $LWO_2(OH)$ in acetonitrile reacted with butyllithium (pK_b ca. −44[51]), aqueous NEt_4OMe (pK_b ca. −15.7), aqueous ammonia (pK_b ca. −9.3), and methanol solutions of sodium phenolate (pK_b ca. −9.9), sodium thiophenolate (pK_b ca. −6.5), and sodium acetate (pK_b ca. −4.8), with solubilization and anion formation according to eq 5. No change in suspensions of $LWO_2(OH)$ in acetonitrile was observed upon the addition of weaker bases such as aniline (pK_b ca. −4.6), methanol solutions of sodium formate (pK_b ca. −3.8), or acetamide (pK_b ca. 0.37). Solutions of $NEt_4[LWO_3]$ (vide infra) in acetonitrile did not precipitate insoluble $LWO_2(OH)$ over a period of 1 month after addition of phenol or thiophenol. However, $LWO_2(OH)$ was precipitated from acetonitrile upon addition of glacial acetic acid or hydrochloric acid. These observations permit the pK_a of $LWO_2(OH)$ to be estimated at 4.6−4.8.

Schreiber et al.[24,25] have described the only other hydroxodioxotungsten(VI) complex, i.e., $[(Me_3tcn)W^{VI}O_2(OH)]Br$, formed upon reaction of $(Me_3tcn)W^{VI}O_3$ with concentrated hydrobromic acid. This complex exhibits $\nu(WO_2)$ absorptions at 951 and 914 cm^{-1} and a band assigned to the ν(W−OH) absorption at 698 cm^{-1}. In the solid state, the hydroxo ligand of the complex cation and a bromide counteranion are involved in a hydrogen bond characterized by an O(H)··Br distance of 3.08 Å. While we were unable to grow crystals of $LWO_2(OH)$ suitable for an X-ray diffraction study, it is reasonable to suppose that the compound's solid state structure may be strongly influenced by intermolecular hydrogen bonds of the W−OH··O═W type. Related $Cp^*MO_2(OH)$[26] (M = Mo, W) and $LMoO_2(OH)$[52] complexes are proposed as intermediates in the formation of $[Cp^*MO_2]_2(\mu\text{-}O)$ and $[LMoO_2]_2(\mu\text{-}O)$, respectively, but are too unstable to be isolated. Transient $(Bu^tCH_2)_3WO(OH)$ is also unstable with respect to condensation to $[(Bu^tCH_2)_3WO]_2(\mu\text{-}O)$.[22]

Synthesis and Characterization of $NEt_4[LWO_3]\cdot 4H_2O$. Reaction of a suspension of $LWO_2(OH)$ in acetonitrile with 1 equiv of NEt_4OMe resulted in the formation of a solution of $NEt_4[LWO_3]$. Evaporation of the solvent and recrystallization from CH_2Cl_2/diethyl ether provided a 92% yield of the tetrahydrate, $NEt_4[LWO_3]\cdot 4H_2O$. The colorless, diamagnetic compound is indefinitely stable in the solid state and in solution. It is extremely soluble in CH_2Cl_2, MeCN, and MeOH, appreciably soluble in water, but insoluble in diethyl ether and alkanes.

Microanalytical data were consistent with the tetrahydrate formulation. Positive-ion fast-atom-bombardment mass spectra

(48) Wolowiec, S.; Kochi, J. K. *Inorg. Chem.* **1991**, *30*, 1215.
(49) Pinchas, S.; Laulicht, I. *Infrared Spectra of Labelled Compounds*; Academic Press: London, 1971.
(50) Kramarz, K. W.; Norton, J. R. *Prog. Inorg. Chem.* **1994**, *42*, 1.
(51) The pK_b values are derived from the pK_a values for the corresponding free acids, from data obtained from: (a) Dean, J. A. *Lange's Handbook of Chemistry*, 14th ed.; McGraw-Hill: New York, 1992; Table 8.8. (b) Gordon, A. J.; Ford, R. A. *The Chemist's Companion*; Wiley: New York, 1972; pp 58−63.
(52) Xiao, Z.; Enemark, J. H.; Wedd, A. G.; Young, C. G. *Inorg. Chem.* **1994**, *33*, 3438.

Table 3. Selected Distances and Angles for $NEt_4[LWO_3]\cdot 4H_2O$[a]

	Bond Distances (Å)		
W−O(1)	1.740(4)	W−O(2)	1.759(4)
W−O(3)	1.765(4)	W−N(11)	2.339(4)
W−N(21)	2.332(5)	W−N(31)	2.308(5)
	Hydrogen-Bond Distances (Å)		
O(2)···O(5)^{i}	2.666(6)	O(3)···O(4)^{ii}	2.693(6)
O(4)···O(7)^{iii}	2.833(7)	O(4)···O(6)^{i}	2.851(7)
O(4)···O(6)^{iv}	2.897(7)	O(5)···O(7)^{i}	2.853(8)
O(5)···O(6)^{iii}	2.870(8)	O(5)···O(7)	2.901(7)
	Angles (deg)		
O(1)−W−O(2)	103.8(2)	O(1)−W−O(3)	104.8(2)
O(2)−W−O(3)	104.5(2)	O(1)−W−N(11)	160.4(2)
O(1)−W−N(21)	86.9(2)	O(1)−W−N(31)	88.6(2)
O(2)−W−N(11)	87.6(2)	O(2)−W−N(21)	160.9(2)
O(2)−W−N(31)	88.4(2)	O(3)−W−N(11)	87.3(2)
O(3)−W−N(21)	87.6(2)	O(3)−W−N(31)	158.2(2)
N(11)−W−N(21)	78.2(2)	N(11)−W−N(31)	75.6(2)
N(21)−W−N(31)	75.9(2)	W−O(2)···O(5)^{i}	156.1(3)
W−O(3)···O(4)^{ii}	139.0(2)		

[a] Symmetry operations: (i) $1-x, -y, 1-z$; (ii) $x, 0.5-y, 0.5+z$; (iii) $x, 0.5-y, -0.5+z$; (iv) $x, y, -1+z$.

featured a peak cluster at *m/z* 789, which was assigned to the $\{(NEt_4)_2[LWO_3]\}^+$ aggregate ion. The infrared spectrum of $NEt_4[LWO_3]\cdot 4H_2O$ exhibited bands characteristic of L, NEt_4^+, and water of crystallization. As well, three strong bands at 920, 860, and 825 cm^{-1} were assigned to the A′, A′ and A″ $\nu(WO_3)$ vibrations, respectively, of a WO_3 fragment with local C_s symmetry. Two modes ($A_1 + E$) are predicted for an idealized $[LWO_3]^-$ anion of C_{3v} symmetry, but hydrogen bonding involving two of the oxo ligands (vide infra) reduces the local symmetry of the anion to C_s. In chloroform solution, two bands corresponding to the A_1 (920 cm^{-1}) and E (840 cm^{-1}) modes of a C_{3v} trioxo anion were observed. According to the treatment described by Burdett,[53] the intensity ratio of these bands is related to the angle γ that the W═O vectors make with the plane perpendicular to the C_3 axis by eq 6, where I_s and I_a are the intensities of the A_1 and E modes, respectively. For

$$\tan^2 \gamma = I_s/I_a \qquad (6)$$

$[LWO_3]^-$ in chloroform solution, a γ angle of 22° was calculated using this treatment, in good agreement with a γ angle of 24° estimated from the crystal structure of $NEt_4[LWO_3]\cdot 4H_2O$ (vide infra). The observation of two $\nu(MoO_3)$ bands in the infrared spectrum of $NEt_4[(HB(pz)_3)MoO_3]$ and three in the spectrum of $NEt_4[(HB(pz)_3)MoO_3]\cdot 2H_2O$ has been attributed to the effects of hydrogen bonding.[48] The ^1H NMR spectrum of $NEt_4[LWO_3]\cdot 4H_2O$ exhibited three resonances assignable to L [δ 2.28 (9H), 2.83 (9H), 5.72 (3H)], the characteristic triplet of triplet and quartet resonances of the NEt_4^+ cation, and a water resonance at δ 2.05. The NMR spectrum is consistent with the molecular C_{3v} symmetry of the anion in solution. Similar ligand resonances [2.26 (9H), 2.83 (9H), 5.66 (3H)] have been reported for the anion in $(Ph_3POH)[LWO_3]\cdot 2H_2O$.[28]

Crystal Structure of $NEt_4[LWO_3]\cdot 4H_2O$. The crystal structure of $NEt_4[LWO_3]\cdot 4H_2O$ is composed of discrete NEt_4^+ and *fac*-$[LWO_3]^-$ ions, arranged in an alternating fashion on both sides of a zigzag ladder of hydrogen-bonded water molecules directed parallel to the *b* axis of the unit cell; selected interatomic parameters are collected in Table 3. In the distorted-octahedral anion (Figure 1), the tungsten atom is coordinated by a facially tridentate L ligand and three terminal oxo ligands, with W−O(1) = 1.740(4) Å, W−O(2) = 1.759(4) Å, and

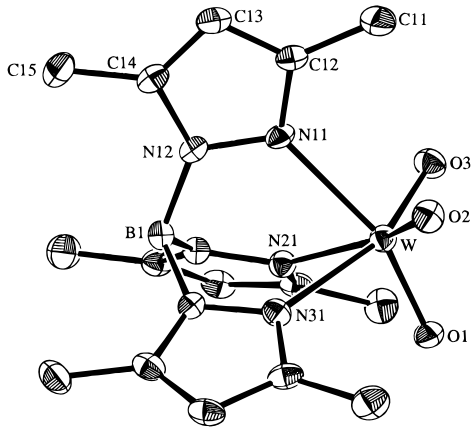

Figure 1. Molecular structure of the anion in $NEt_4[LWO_3]\cdot 4H_2O$. The numbering schemes of the pyrazole rings containing N(21) and N(31) parallel that shown for the ring containing N(11).

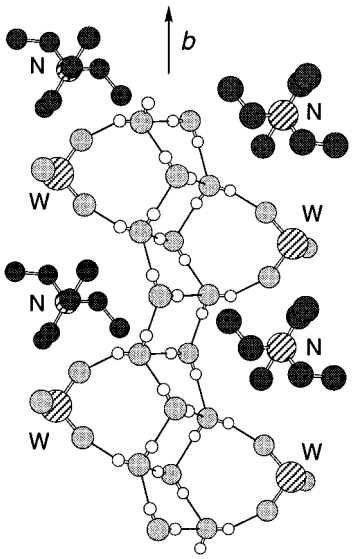

Figure 2. Partial structure of $NEt_4[LWO_3]\cdot 4H_2O$ showing the arrangement of cations and anions along the crystallographic *b* axis and the nature of the hydrogen bonding in the zigzag ladder of water molecules. For clarity, only the WO_3 fragment of each anion is shown. The missing L ligands occupy the regions of space bounded by the NEt_4^+ cations and the water network.

W−O(3) = 1.765(4) Å. The WO_3 unit is compressed along the pseudo-3-fold axis while the WN_3 unit is elongated along the same axis. Consequently, the W atom lies only 0.7196(2) Å out of the plane defined by the O(1), O(2), and O(3) atoms, while W lies 1.6254(2) Å out of the plane defined by the three N(*n*1) atoms. The distortion is also reflected in the angles that the W−O and W−N bonds subtend with the pseudo-3-fold axis,[54] ca. 66 and 136°, respectively, and the average O(*n*)−W−N(*n*1) angle of 159.8(1)°. The O−W−O angles are an average 104.4(1)°, which is typical of related WO_3 and $[WO_2]^{2+}$ complexes. The W−N(*n*1) distances, which range from 2.308(5) Å for W−N(31) to 2.339(4) Å for W−N(11), are dictated by the relative *trans* influences of the oxo ligands. The array of cations and anions along the zigzag ladder of hydrogen-bonded water molecules is displayed in Figure 2. The anion is hydrogen-bonded to the ladder of water molecules via the O(2) and O(3) atoms, with WO(2)··O(5)^{i} and WO(3)··O(4)^{ii} separations of 2.666(6) and 2.693(6) Å, respectively (see Table 3 for symmetry operations). These O··O separations are less than

(53) Burdett, J. K. *Inorg. Chem.* **1981**, *20*, 2607.

(54) Here, we refer to the angles the W→O and W→N vectors make with the pseudo-C_3 axis (the B→W vector defines the positive direction of the axis).

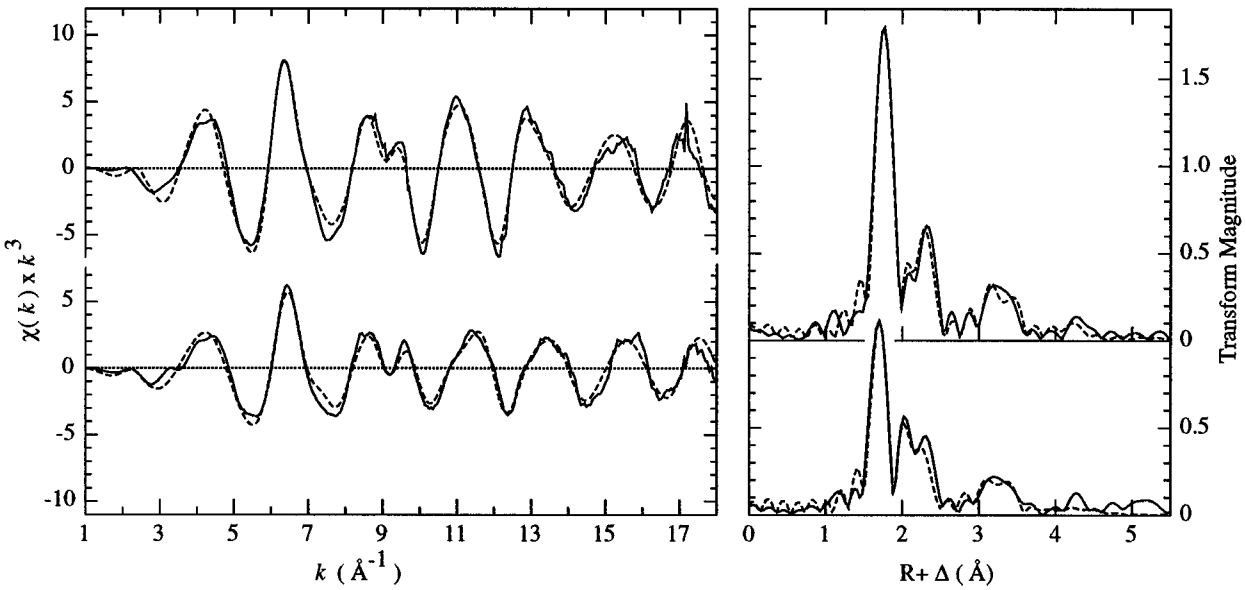

Figure 3. EXAFS curve-fitting results. The left panel shows the EXAFS spectra (solid lines) and best fits (dashed lines) for $NEt_4[LWO_3]\cdot 4H_2O$ (top) and $LWO_2(OH)$ (bottom). The right panel shows the EXAFS Fourier transforms (solid lines) and best fits (dashed lines), phase-corrected for W−O backscattering, for $NEt_4[LWO_3]\cdot 4H_2O$ (top) and $LWO_2(OH)$ (bottom).

those of the ice-I_h hexagonal structure (O··O = 2.752−2.765 Å),[55] consistent with the highly basic character of the oxo ligands. The O(1) atom does not take part in any hydrogen-bond interactions but points directly toward a pyrazole ring in an adjacent anion. The slight lengthening of the W−O(2) and W−O(3) bonds versus the W−O(1) bond may be ascribed to the influence of this hydrogen bonding. In the ladder structure, the O···O separations range from 2.833(7) to 2.901(7) Å and are typical of hydrogen-bond interactions of this type.[56,57] In the model for the hydrogen bonding presented in Figure 2, the rungs of the ladder are formed by water molecules which do not interact with the W═O groups. However, the hydrogen atoms were not located in the X-ray diffraction study and the possibility of other hydrogen-bonding motifs must be acknowledged.

Hydrogen bonding is a feature of hydrated metal oxides[58] and many trioxo−metal complexes. Trioxotungsten complexes exhibit hydrogen bonding to countercations, e.g., $[Bu^tNH_3][Cp^*WO_3]$,[22] water and coligands, e.g., $(tcn)WO_3\cdot 3H_2O$, where all three oxo ligands are hydrogen-bonded to water or a combination of water and N−H groups from tcn,[24,25] or simply waters of crystallization, e.g., $[N(PPh_3)_2][Cp^*WO_3]\cdot 2H_2O$.[22] All three oxo ligands of the distorted-octahedral anion in $NEt_4[(HB(pz)_3)MoO_3]\cdot 2H_2O$ are involved in localized hydrogen bonds involving the waters of crystallization.[48] The level of hydration of $NEt_4[LMoO_3]$ was not specified,[48] and it is unclear whether its structure is related to that described above for $NEt_4[LWO_3]\cdot 4H_2O$. The synthesis of $[Ph_3POH][LWO_3]$ via hydrolysis of $LWO_2(CHPPh_3)$ was recently described by Sundermeyer et al.;[28] the compound crystallizes as the dihydrate but has not been structurally characterized. A number of closely related polypyrazolylborate trioxorhenium[59,60] and -technetium[61] complexes have been described.

The basicity of trioxo−metal fragments is evident from their propensity to participate in hydrogen bonding and nucleophilic reactions. The protonation of $[LWO_3]^-$ (vide supra) and $(Me_3tcn)WO_3$[23,24] and the formation of complexes such as $[M\{(\mu\text{-}O)WO_2(tcn)\}_6]^{2+}$ when $(tcn)WO_3$ reacts with the Lewis acids $M^{2+}(aq)$ (M = Co, Fe)[22,23] provide examples of this behavior in tungsten chemistry. The Brønsted and Lewis base character of $[LWO_3]^-$ and related complexes is consistent with considerable localization of electronic charge on the terminal oxo ligands. A recently published[62] Mulliken analysis for $RReO_3$ complexes, which showed considerable electron density on the oxo ligands, provides specific support for this general view.

EXAFS. Tungsten L_{III}-edge XAS measurements were performed on $LWO_2(OH)$ and $NEt_4[LWO_3]\cdot 4H_2O$ and, for comparison purposes, on the closely related tri-N-donor complexes $(dien)WO_3$, $(Me_3tcn)WO_3$, $[(Me_3tcn)WO_2(OH)]Br$, and $LWO_2(OMe)$. Figure 3 shows the EXAFS spectra, the best fits, and the corresponding Fourier transforms for $LWO_2(OH)$ and $NEt_4[LWO_3]\cdot 4H_2O$. The results of the curve-fitting analyses are given in Table 2. The results we now describe provide strong evidence to support the formulations of the title complexes. For $NEt_4[LWO_3]\cdot 4H_2O$, the Fourier transform showed only two major peaks, corresponding to the W═O and W−N interactions. Small outer-shell features associated with the presence of L were also present. The overall best fit to the EXAFS was obtained with three oxo ligands at 1.766(3) Å and three nitrogen donor atoms at 2.314(8) Å. These values are in good agreement with the values obtained from the X-ray structure of this compound. In contrast, $LWO_2(OH)$ showed three peaks arising from W═O and W−O/N backscattering in the EXAFS Fourier transform (EXAFS cannot readily distinguish scatterers of similar atomic number). In this case, best fits were obtained with two oxo ligands [W═O = 1.736(4) Å], a single hydroxo ligand [W−O = 1.903(10) Å], and three W−N interactions [W−N = 2.256(10) Å]. A definitive statement concerning the location of the "proton" in $LWO_2(OH)$ (or LWO_3H) depends critically on the number and type of oxygen

(55) Peterson, S. W.; Levy, H. A. *Acta Crystallogr.* **1957**, *10*, 70.
(56) Reference 2, p 635.
(57) Pimentel, G. C.; McClellan, A. L. *The Hydrogen Bond*; Freeman: San Francisco, CA, 1960.
(58) For example, $MoO_3\cdot 2H_2O$: Krebs, B. *Acta Crystallogr.* **1972**, *B28*, 2222.
(59) Degnan, I. A.; Herrmann, W. A.; Herdtweck, E. *Chem. Ber.* **1990**, *123*, 1347.
(60) Domingos, A.; Marcalo, J.; Paulo, A.; de Matos, A. P.; Santos, I. *Inorg. Chem.* **1993**, *32*, 5114.
(61) Thomas, J. A.; Davison, A. *Inorg. Chim. Acta* **1991**, *190*, 231.
(62) Köstlmeier, S.; Häberlen, O. D.; Rösch, N.; Herrmann, W. A.; Solouki, B.; Bock, H. *Organometallics* **1996**, *15*, 1872.

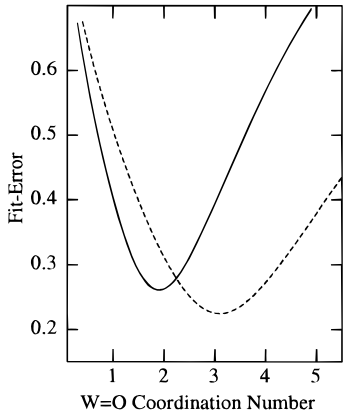

Figure 4. Search profiles for W═O coordination numbers for $NEt_4[LWO_3]\cdot 4H_2O$ (dashed line) and $LWO_2(OH)$ (solid line). Search profiles were calculated by refining all parameters except for coordination numbers, which were systematically varied over the range shown on the abscissa of the plots.

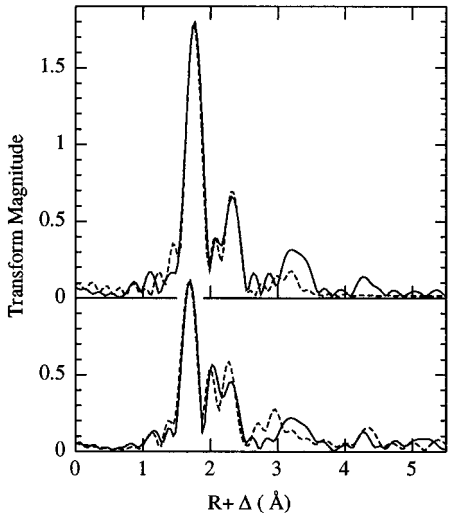

Figure 5. Comparison of EXAFS Fourier transforms. Top: $NEt_4[LWO_3]\cdot 4H_2O$ (solid line) and $(Me_3tcn)WO_3$ (dashed line). Bottom: $LWO_2(OH)$ (solid line) and $[(Me_3tcn)WO_2(OH)]Br$ (dashed line).

ligands detected. Figure 4 shows search profiles for the W═O coordination numbers, for which other parameters (i.e., bond lengths and Debye−Waller factors) were allowed to float freely, and the resulting goodness of fit is plotted against coordination number. Well-defined minima were observed at three and two W═O ligands for $NEt_4[LWO_3]\cdot 4H_2O$ and $LWO_2(OH)$, respectively. Analysis of the EXAFS of closely related complexes further strengthens our confidence in these EXAFS results. Related trioxotungsten complexes, viz., $(dien)WO_3$ and $(Me_3tcn)WO_3$, exhibited two-feature EXAFS Fourier transforms quite analogous to that of $NEt_4[LWO_3]\cdot 4H_2O$ (Figure 5). On the other hand, the EXAFS Fourier transforms of structurally characterized $[(Me_3tcn)WO_2(OH)]Br$ (Figure 5) and $LWO_2(OMe)$ revealed three features as observed for $LWO_2(OH)$. The EXAFS best fits for these compounds were consistent with available structural data or expectations for (O-donor)dioxotungsten(VI) complexes. For example, the EXAFS-derived W−O distance of 1.877(18) Å for $[(Me_3tcn)WO_2(OH)]Br$ compares well with that established by X-ray crystallography [1.893(1) Å], and a similar W−O distance pertains to $LWO_2(OH)$. A comparison of the EXAFS Fourier transforms for pairs of related compounds in Figures 3 and 5 highlights the parallels within and contrasts between the EXAFS and structures of these two classes of compound.

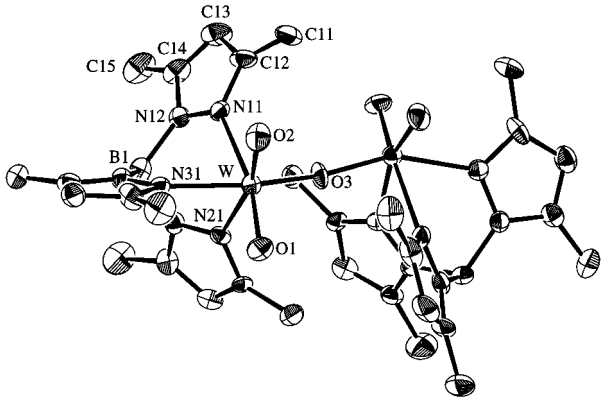

Figure 6. Molecular structure of $[LWO_2]_2(\mu\text{-O})$. The numbering schemes of the pyrazole rings containing N(21) and N(31) parallel that shown for the ring containing N(11).

Synthesis and Characterization of $[LWO_2]_2(\mu\text{-O})$. Reaction of $LWO_2(\mu\text{-O})WO(CO)L$ with Bu^tOOH and iodine in chloroform produced modest yields of cream-colored, diamagnetic $[LWO_2]_2(\mu\text{-O})$. A bright yellow, paramagnetic byproduct of this reaction, tentatively identified as $LWO_2(\mu\text{-O})WOIL$, was conveniently removed by slow recrystallization.[63] It is possible that this byproduct was converted to $[LWO_2]_2(\mu\text{-O})$ in wet, oxygenated methanol, thus explaining the effectiveness of the slow crystal growth used to purify the product. Significant amounts of $[LWO_2]_2(\mu\text{-O})$ also form when LWO_2Cl[14] reacts with PPh_3 in refluxing pyridine and when complexes such as LWO_2X [X = SPh, (−)-mentholate] are synthesized via metathesis of LWO_2Cl and group 1 salts M^IX.[18] It also forms in high yields (by ^1H NMR) from the decomposition of $LWO_2(SePh)$ in undried dichloromethane.[18] The dinuclear complex is very air-stable in the solid state and solution and is soluble in chlorinated solvents but insoluble in alcohols, diethyl ether, and alkanes. Moreover, we have not been able to induce the interconversion of $[LWO_2]_2(\mu\text{-O})$ and the previously described mononuclear species. We have already commented on the stability of solutions of $LWO_2(OH)$ and $NEt_4[LWO_3]$, which under no conditions convert to the dinuclear species. In contrast, the interconversion of $[Cp^*MO_2]_2(\mu\text{-O})$ and $[Cp^*MO_3]^-$ complexes has been reported.[27]

The formula of $[LWO_2]_2(\mu\text{-O})$ was established by microanalysis and fast-atom-bombardment mass spectrometry (*m/z* 1042 (4%) for $[M]^+$). The infrared spectrum contained bands attributable to ν(BH) (2545 cm^{-1}), $\nu_s(WO_2)$ (945 cm^{-1}), $\nu_{as}(WO_2)$ (900 cm^{-1}), and ν_{as}(WOW) (780 cm^{-1}) vibrational modes. The ^1H NMR spectrum exhibited nine resonances attributable to the methyl (6 × 6H) and methine (3 × 2H) groups of L in a dinuclear complex with C_2 or C_i solution symmetry; it is likely that the solid-state structure with C_2 symmetry (vide infra) is retained in solution. Two unusual methyl resonances were observed, one shielded (δ 1.10) and the other reasonably deshielded (δ 3.22), as a result of the composite shielding effects of pyrazole and W═O groups. The analogous molybdenum complex is characterized by comparable spectroscopic properties: $\nu(MoO_2)$ 931 and 900 cm^{-1} and nine NMR resonances with outlying methyl resonances at δ 1.07 and 3.09.[52]

Crystal Structure of $[LWO_2]_2(\mu\text{-O})$. The molecular structure of $[LWO_2]_2(\mu\text{-O})$ is composed of two six-coordinate, distorted-octahedral tungsten centers bridged by a μ-oxo ligand (Figure 6); selected parameters are collected in Table 4. Each tungsten atom is coordinated by a facially tridentate L ligand,

(63) Related Mo complexes that have been isolated exhibit similar properties: (a) Eagle, A. A.; Mackay, M. F.; Young, C. G. *Inorg. Chem.* **1991**, *30*, 1425. (b) Reference 52.

Table 4. Selected Bond Distances and Angles for $[LWO_2]_2(\mu\text{-}O)^a$

		Bond Distances (Å)	
W−O(1)	1.715(5) [1.701(2)]	W−O(2)	1.715(5) [1.696(2)]
W−O(3)	1.893(1) [1.889(1)]	W−N(11)	2.317(6) [2.318(2)]
W−N(21)	2.317(6) [2.314(2)]	W−N(31)	2.198(6) [2.208(2)]
		Bond Angles (deg)	
O(1)−W−O(2)	102.8(3) [102.7(1)]	O(1)−W−O(3)	102.8(2) [102.5(1)]
O(2)−W−O(3)	102.6(3) [104.11(9)]	O(1)−W−N(11)	164.7(3) [165.34(9)]
O(1)−W−N(21)	86.9(3) [87.82(9)]	O(1)−W−N(31)	92.9(2) [90.14(9)]
O(2)−W−N(11)	88.3(3) [85.83(8)]	O(2)−W−N(21)	164.9(2) [164.32(8)]
O(2)−W−N(31)	90.4(3) [91.42(9)]	O(3)−W−N(11)	84.7(1) [86.57(9)]
O(3)−W−N(21)	86.2(3) [84.50(5)]	O(3)−W−N(31)	156.7(2) [157.02(7)
N(11)−W−N(21)	80.3(3) [81.59(7)]	N(11)−W−N(31)	76.3(2) [77.64(7)]
N(21)−W−N(31)	77.5(2) [76.82(8)]	W−O(3)−W′	167.0(5) [167.1(2)]

[a] For comparison, data pertaining to the structure of $[LMoO_2]_2(\mu\text{-}O)$[65] are given in square brackets.

two terminal oxo ligands, and a corner-shared μ-oxo ligand. A crystallographically imposed C_2 axis passes through the bridging oxo ligand. The W═O bond lengths, which are identical at 1.715(5) Å, are typical of *cis*-dioxotungsten(VI) complexes. The bridging W−O(3) bond distance is longer at 1.893(1) Å and is somewhat shorter than the average (1.916 Å) for μ-oxo-bridged tungsten complexes.[64] The O(1)−W−O(2) bond angle of 102.8(3)° is close to angles subtended by *cis* oxo ligands in other complexes.[5,14,18] A W−O−W′ bond angle of 167.0(5)° is observed. The W−N(11) and W−N(21) bonds *trans* to the teminal oxo ligands are longer, at 2.317(6) Å, than the W−N(31) bond *trans* to the bridging oxo group, at 2.198(6) Å, consistent with the *trans* influences of the ligands. The entirely analogous structure of $[LMoO_2]_2(\mu\text{-}O)$ has been reported by Barnhart and Enemark;[65] some structural parameters are listed in Table 4. A comparison of the derived interatomic parameters for the two structures reveals that many are equal within experimental error, suggesting that the substitution of W for Mo has only a small influence on the overall structure. Related structures have been described for the dinuclear complexes $[\{(tcn)WO_2\}_2(\mu\text{-}O)](S_2O_6)\cdot 4H_2O$,[24,25] with average W═O and W−O distances of 1.755 and 1.896 Å and a W−O−W angle of 157.9°, and $Na_6[\{WO_2(citrate)\}_2(\mu\text{-}O)]\cdot 10H_2O$,[19,32] with average W═O and W−O distances of 1.757 and 1.893 Å and a W−O−W angle of 180°. The structure of $[LWO_2]_2(\mu\text{-}O)$ is only the third described for dinuclear (μ-oxo)bis[dioxotungsten(VI)] complexes. The closest intermolecular contact in the lattice involving the non-H atoms occurs between the O(2) and C(13)′ atoms at 3.36(1) Å (symmetry operation: x, $1 + y$, z).

Summary

The synthesis and characterization of the principal binary oxotungsten(VI) complexes of hydrotris(3,5-dimethylpyrazol-1-yl)borate have been described. The complexes may be accessed by a variety of low-valent and high-valent synthetic approaches and have been characterized by a wide range of techniques, including EXAFS spectroscopy and X-ray diffraction. The $LWO_2(OH)$ complex is stable toward condensation, but its weak acidity permits deprotonation to salts of the corresponding anion, $[LWO_3]^-$. These two mononuclear W(VI) complexes are not converted to the dinuclear complex $[LWO_2]_2(\mu\text{-}O)$. Further developments in the oxotungsten(VI) chemistry of hydrotris(3,5-dimethylpyrazolyl)borate[18] will be the subject of future papers.

Acknowledgment. A.A.E. and C.G.Y. thank the Australian Department of Industry, Science, and Technology for a travel grant permitting XAS measurements at SSRL, Dr. L. Spiccia for a gift of tcn·3HCl, and Mr. S. Thomas for experimental assistance. Financial support from the Australian Research Council and the National Institutes of Health is gratefully acknowledged.

Supporting Information Available: Two X-ray crystallographic files in CIF format are available on the Internet only. Access information is given on any current masthead page.

IC9609261

(64) Orpen, A. G.; Brammer, L.; Allen, F. H.; Kennard, O.; Watson, D. G.; Taylor, R. *J. Chem. Soc., Dalton Trans.* **1989**, S1.

(65) Barnhart, K. M.; Enemark, J. H. *Acta Crystallogr.* **1984**, *C40*, 1362.